tvst

DOI: 10.1167/tvst.1.2.5

Article

Imaging Retinal Vascular Changes in the Mouse Model of Oxygen-Induced Retinopathy

João M. Furtado[1], Michael H. Davies[1], Dongseok Choi[2], Andreas K. Lauer[1], Binoy Appukuttan[1], Steven T. Bailey[1], Hassan T. Rahman[3], John F. Payne[3], Andrew J. Stempel[1], Kathleen Mohs[1], Michael R. Powers[1,4], Steven Yeh[3], and Justine R. Smith[1,5] ✉

[1] Casey Eye Institute, Oregon Health & Science University, Portland, OR
[2] Department of Public Health & Preventive Medicine, Oregon Health & Science University, Portland, OR
[3] Department of Ophthalmology, Emory Eye Center, Emory University, Atlanta, GA
[4] Department of Pediatrics, Oregon Health & Science University, Portland, OR
[5] Department of Cell & Developmental Biology, Oregon Health & Science University, Portland, OR

Correspondence: Justine R. Smith, Oregon Health & Science University, Mail Code L467AD, Biomedical Research Building, 3181 S.W. Sam Jackson Park Road, Portland, OR 97239, USA. e-mail: smithjus@ohsu.edu

Received: 17 June 2012
Accepted: 4 August 2012
Published: 18 September 2012

Keywords: retinopathy of prematurity, oxygen-induced retinopathy, retina, imaging

Citation: Furtado JM, et al. Imaging retinal vascular changes in the mouse model of oxygen-induced retinopathy. Trans Vis Sci Tech. 2012; 1(2):5, http://tvstjournal.org/doi/full/10.1167/tvst.1.2.5, doi:10.1167/tvst.1.2.5

Purpose: Oxygen-induced retinopathy in the mouse is the standard experimental model of retinopathy of prematurity. Assessment of the pathology involves in vitro analysis of retinal vaso-obliteration and retinal neovascularization. The authors studied the clinical features of oxygen-induced retinopathy in vivo using topical endoscopy fundus imaging (TEFI), in comparison to standard investigations, and evaluated a system for grading these features.

Methods: Postnatal day (P)7 mice were exposed to 75% oxygen for five days to induce retinopathy or maintained in room air as controls. Retinal vascular competence was graded against standard photographs by three masked graders. Retinal photographs were obtained at predetermined ages using TEFI. Postmortem, retinal vaso-obliteration was measured in whole mounts with labeled vasculature, and retinal neovascularization was quantified in hematoxylin- and eosin-stained ocular cross sections.

Results: Fundus photography by TEFI was possible from P15, when retinal vascular incompetence, including dilatation and tortuosity, was significant in mice with oxygen-induced retinopathy in comparison to controls. Vascular incompetence peaked in severity at P17 and persisted through P25. Comparison with in vitro analyses indicated that vascular changes were most severe after retinal avascularity had begun to decrease in area, and coincident with the maximum of retinal neovascularization. A weighted Fleiss-Cohen kappa indicated good intra- and interobserver agreement for a 5-point grading system.

Conclusions: Topical endoscopy fundus imaging demonstrates retinal vascular incompetence in mice with oxygen-induced retinopathy. The technique complements standard postmortem analysis for following the course of the model.

Translational Relevance: Topical endoscopy fundus imaging has application in the evaluation of novel biologic drugs for retinopathy of prematurity.

Introduction

Retinopathy of prematurity is an ischemic vasculopathy affecting premature neonates.[1] The vasculopathy is most sight threatening when retinal neovascularization occurs and is complicated by vitreous hemorrhage and/or retinal detachment. Across the globe, retinopathy of prematurity is the cause of blindness for more than 50,000 children, the majority of whom live in low- and middle-income countries.[2] Yet the quoted prevalence of blindness provides a gross underestimate of the public health impact of the disease, as a blind child lives many years with the disability,[3] and a considerably larger number

of affected children suffer visual impairment or unilateral blindness.[2] For this reason, retinopathy of prematurity has been identified as a priority eye disease by the World Health Organization.[4] Treatment of the vasculopathy is typically considered when retinal neovascularization and/or marked vascular incompetence develop behind the nasal ora serrata, that is, "type 1 prethreshold" retinopathy.[5,6] Ablation of avascular peripheral retina is recommended, which is most commonly performed by laser photocoagulation and less frequently by transscleral cryotherapy. Such treatment is highly effective, but carries risks of structural complications.[7] Drugs targeting the major angiogenic regulator in retinal neovascularization—vascular endothelial growth factor (VEGF)—may induce regression of new vessels. However, use is controversial due to concerns of systemic toxicity and possible impact on normal ocular development.[8] These issues explain the high level of research activity focused on the development of new drugs for retinopathy of prematurity.

Animal models are instrumental in the identification of potential therapeutic targets in retinopathy of prematurity and for testing novel medical interventions. The mouse model of oxygen-induced retinopathy, which was developed in the 1990s,[9] has been used extensively to study mechanisms of retinopathy of prematurity and other retinal ischemic vasculopathies.[10] In this model, 7-day-old mouse pups are placed in 75% oxygen for five days and subsequently transferred into room air.[9] Several practical reasons explain the success of mouse oxygen-induced retinopathy as an experimental model, as have been well summarized,[11] including incomplete retinal vascularization in the mouse at birth; the large variety of genetically engineered mutants; and relatively low animal husbandry costs. In addition and most importantly, two histopathological hallmarks of retinopathy of prematurity are recapitulated in oxygen-induced retinopathy, namely retinal vaso-obliteration and retinal neovascularization. Standard assessment of these two features of the disease involves postmortem evaluation of retinal whole mounts and/or ocular cross sections.[10,12] On the other hand, clinical aspects of oxygen-induced retinopathy in the mouse remain unexplored.

In human neonates, retinopathy of prematurity is evaluated by indirect ophthalmoscopy and using descriptors that include location, extent, and severity.[13] An inexpensive, noninvasive ophthalmoscopic method, topical endoscopy fundus imaging (TEFI), was recently described as a method for obtaining high-resolution digital photographic images of the posterior pole of live mice.[14] This technique has already been employed successfully to study clinical aspects of posterior uveitis in the mouse.[15,16] We used TEFI to characterize the clinical features of mouse oxygen-induced retinopathy, and to evaluate a simple grading system for following the severity of disease across critical postnatal ages. In addition, we correlated our clinical findings with the traditional methods used to score retinal vaso-obliteration and retinal neovascularization.

Methods

Animals

Breeding pairs of C57BL/6 mice were originally purchased from The Jackson Laboratory (Bar Harbor, ME). All mice were provided food and water ad libitum and kept on a 12-hour light/dark cycle. Experiments were designed and performed in accordance with the guidelines of the ARVO Statement for the Use of Animals in Ophthalmic and Vision Research and with the approval of the Institutional Animal Care and Use Committee of Oregon Health & Science University.

Oxygen-Induced Retinopathy in Mice

Oxygen-induced retinopathy was induced in C57BL/6 pups, following the original description.[9] Briefly, postnatal day (P)7 mice, together with nursing females, were exposed to 75% oxygen for five days and then allowed to recover in room air. Age-matched room air control mice were raised under otherwise identical conditions. Mice were grouped according to oxygen exposure (i.e., hyperoxia vs. room air) and age at euthanasia. Ages selected for euthanasia included those typically used to follow the course of disease histopathologically: P12 (peak of retinal vaso-obliteration), P15, P17 (peak of retinal neovascularization), P21, and P25 (resolution of retinal vaso-obliteration and neovascularization).[9] Fundus imaging was performed on both eyes immediately prior to euthanasia. After euthanasia, both eyes were enucleated, and right eyes were processed as retinal whole mounts for vascular staining, while left eyes were embedded whole for sectioning and staining with hematoxylin and eosin.

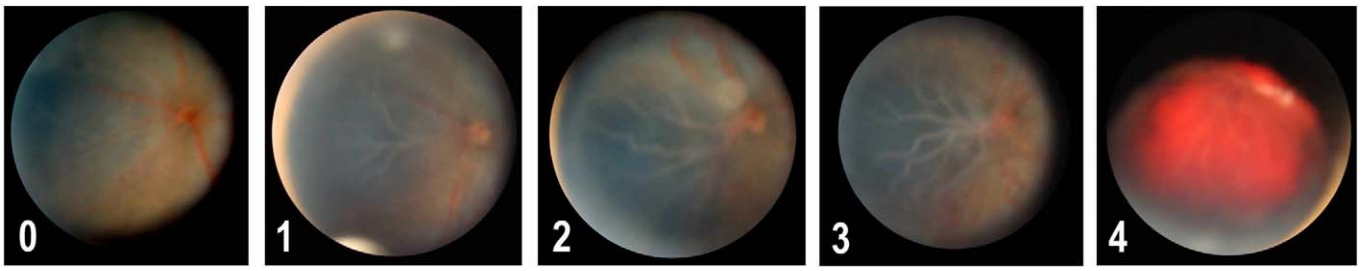

Figure 1. Retinal vascular competence grading system. Grade 0 = No vascular changes. All vessels are narrow and demonstrate a straight course. Grade 1 = Mild vascular changes. Vascular tortuosity is limited to slight undulations of a minority of vessels. Vascular dilation may be present, but involves large vessels alone, and small vessels are difficult to visualize. Grade 2 = Moderate vascular changes. Vascular tortuosity is present in the majority of vessels as obvious undulations. Vascular dilation is always present, and a few small vessels are clearly visible. The white spot about optic disc is a photographic artifact. Grade 3 = Severe vascular changes. Vascular tortuosity is present in the majority of vessels as obvious undulations. Vascular dilatation is extreme, and many small vessels are clearly visible. Grade 4 = Vitreous hemorrhage.

Topical Endoscopic Fundus Imaging

In preparation for imaging, mice were anesthetized by inhalation of isofluorane, followed by pupil dilatation with 2.5% phenylephrine hydrochloride (Bausch & Lomb, Tampa, FL) and 1% tropicamide (Alcon, Fort Worth, TX). Fundus photographs were obtained by TEFI, adapted from reported methods[14,16] using a tripod-mounted Nikon D90 camera (Nikon, Tokyo, Japan), a 60 mm *f*/2.8D lens (Nikon), a 62–52 step-down ring, the Storz 590-44 coupling adaptor (Karl Storz, Tuttlingen, Germany), the Storz 481C halogen light (Karl Storz), and the Storz 1218 tele-otoscope (Karl Storz). Cartoon and photographic images of the equipment appear in the original description.[14] The tele-otoscope was applanated to the cornea after application of Genteal gel (Novartis, East Hanover, NJ). The camera was set to manual focus mode, with 0.1- to 0.2-second shutter speed, *f*/2.8 lens aperture, and ISO 800 for mice aged P21 or older or ISO 1600 for mice aged P17 or younger. At least one photograph of the posterior pole of each retina was obtained from each mouse, and whenever possible, images from superior, nasal, temporal, and inferior retinal peripheries were also obtained. Photographs were saved in RAW mode, and ViewNX2 (Nikon) was used to adjust contrast, brightness, exposure, and white balance, and to convert the images to TIFF files.

The TIFF files were inserted into a single file created in PowerPoint 2007 (Microsoft, Redmond, WA), with images from same eyes montaged, and each retinal representation was masked. Thirty-three percent of all eyes were repeated within this file for the purposes of assessing intragrader variation. Retinal vascular disease was scored in silico over a one-week period by three independent graders, using a 5-point "retinal vascular competence" grading system that was described in a series of standard photographs accompanied by descriptive text (Fig. 1; Grade 0 = No vascular changes. All vessels are narrow and demonstrate a straight course. Grade 1 = Mild vascular changes. Vascular tortuosity is limited to slight undulations of a minority of vessels. Vascular dilation may be present, but involves large vessels alone, and small vessels are difficult to visualize. Grade 2 = Moderate vascular changes. Vascular tortuosity is present in the majority of vessels as obvious undulations. Vascular dilation is always present, and a few small vessels are clearly visible. Grade 3 = Severe vascular changes. Vascular tortuosity is present in the majority of vessels as obvious undulations. Vascular dilatation is extreme, and many small vessels are clearly visible. Grade 4 = Vitreous hemorrhage). The graders included two vitreoretinal surgeons with experience in the evaluation and treatment of infants with retinopathy of prematurity, and one vision scientist who had no such clinical exposure. Graders were encouraged not to assign a score if retinal details were not clear, unless this was related to vitreous hemorrhage, in order to examine the usefulness of vascular competence as a severity measure at different time points. To be considered informative, at least 50% of diseased eyes and 50% of control eyes at any given time point had to be scored by at least two graders.

Evaluation of Vaso-obliteration in Retinal Whole Mounts

Retinal whole mounts were prepared and stained according to a previously published method.[17] In

brief, retina and lens were dissected from the right eye and fixed in 4% paraformaldehyde for 30 minutes at 4°C. Lens was subsequently removed, and the posterior eye cup was incubated overnight at 4°C in Tris-buffered saline (pH 7.5) containing 0.1% bovine serum albumin and 0.4% Triton X-100, with isolectin GS-IB_4 Alexa Fluor 647 (concentration: 4 μg/mL; Invitrogen-Molecular Probes, Eugene, OR) to label endothelial cells, and anti-mouse alpha smooth muscle antibody Cy3 (clone 1A4, dilution: 1:500; Sigma-Aldrich, St. Louis, MO) to identify arteries. After staining, the retina was incised radially and vitreous was removed. Finally the retina was flat mounted with SlowFade Antifade (Invitrogen-Molecular Probes) and imaged via laser scanning confocal microscopy (Fluoview FV1000; Olympus, San Diego, CA). Five images per retina (i.e., one central and four peripheral) were montaged in Adobe Photoshop CS4 (Adobe, Mountain View, CA) and masked. Total and avascular retinal areas were measured using Image-Pro Plus 6.2 (Media Cybernetics, Bethesda, MD). The area of avascular retina was expressed as a percentage of the total retinal area.

Quantification of Retinal Neovascularization in Ocular Cross Sections

Left eyes were formalin-fixed for three hours, paraffin-embedded, and sectioned at 5 μm thickness. Sections were mounted on glass slides (two sections per slide), and every fourth slide was stained with hematoxylin and eosin, and subsequently masked. Retinal neovascularization was quantified by counting the vascular nuclei extending beyond the inner limiting membrane, avoiding hyaloid vessels near the optic disc and lens (15 slides per eye). Results were expressed as average number of neovascular nuclei per ocular cross section.

Statistical Analyses

The Student's *t*-test, two-tailed, was used to compare each of the disease parameters in mice exposed to hyperoxia versus mice exposed to room air. Descriptive statistics were used to compare the changes in the two postmortem severity measures—that is, percentage of retinal vaso-obliteration and average number of neovascular nuclei—with vascular competence grade for right and left eyes, respectively, at the designated time points. Retinal vascular competence score was averaged across the graders for comparison with other outcome measures. To determine intra- and intergrader agreement for vascular competence, a weighted Fleiss-Cohen kappa[18] was used. A weighted kappa was interpreted to indicate good agreement if over 0.60, moderate if between 0.60 and 0.41, and fair if under 0.41.[19] In addition, analysis of variance (ANOVA) was applied at each designated time point to identify significant differences between scores given by the three graders for diseased or control eyes. In all analyses, a significant difference was defined as one yielding a P value less than 0.05.

Results

We used TEFI to obtain photographic images of the retina in mice with oxygen-induced retinopathy and room air–exposed control mice at selected postnatal ages. Evidence of retinal vascular incompetence was seen over the duration of the study in the form of retinal vascular dilatation and tortuosity, and vitreous hemorrhage in extreme disease. Retinal detachment was not observed. Retinal vascular changes were usually symmetrical in severity. They were most readily appreciated at the posterior pole, due to the concentration of retinal vessels at this location, but also were noted in peripheral retina. Changes affected both retinal arterioles and retinal venules. Although the optic nerve was not involved in the clinical pathology, when vascular incompetence was extreme, it became difficult to clearly visualize this structure. It was not possible to appreciate retinal neovascular tufts in the photographs obtained by TEFI. Representative retinal images taken at different ages appear in Figure 2.

At P12, over 50% of the retinal photographs from diseased mice were judged to be nongradable by two or three graders. Thus this time point was not analyzed further. The reasons for the limited view of the retina were small pupil diameter and media opacity related to normal eye development. In addition, since opening of the eyelids is incomplete at P12, it is necessary to slightly retract the end of the otoscope to obtain the clearest image, resulting in a relatively reduced field of view. At P15, when images were readily graded, although imaging of the peripheral retina was limited, mice with oxygen-induced retinopathy presented with significant vascular tortuosity and dilatation in comparison to control mice (grade mean ± standard error of mean in diseased vs. control animals: 2.05 ± 0.11 vs. 0.50 ± 0.17; n = five or six mice per group; $P < 0.0001$; Student's *t*-test). At P17, the peripheral retina was readily visualized, and vascu-

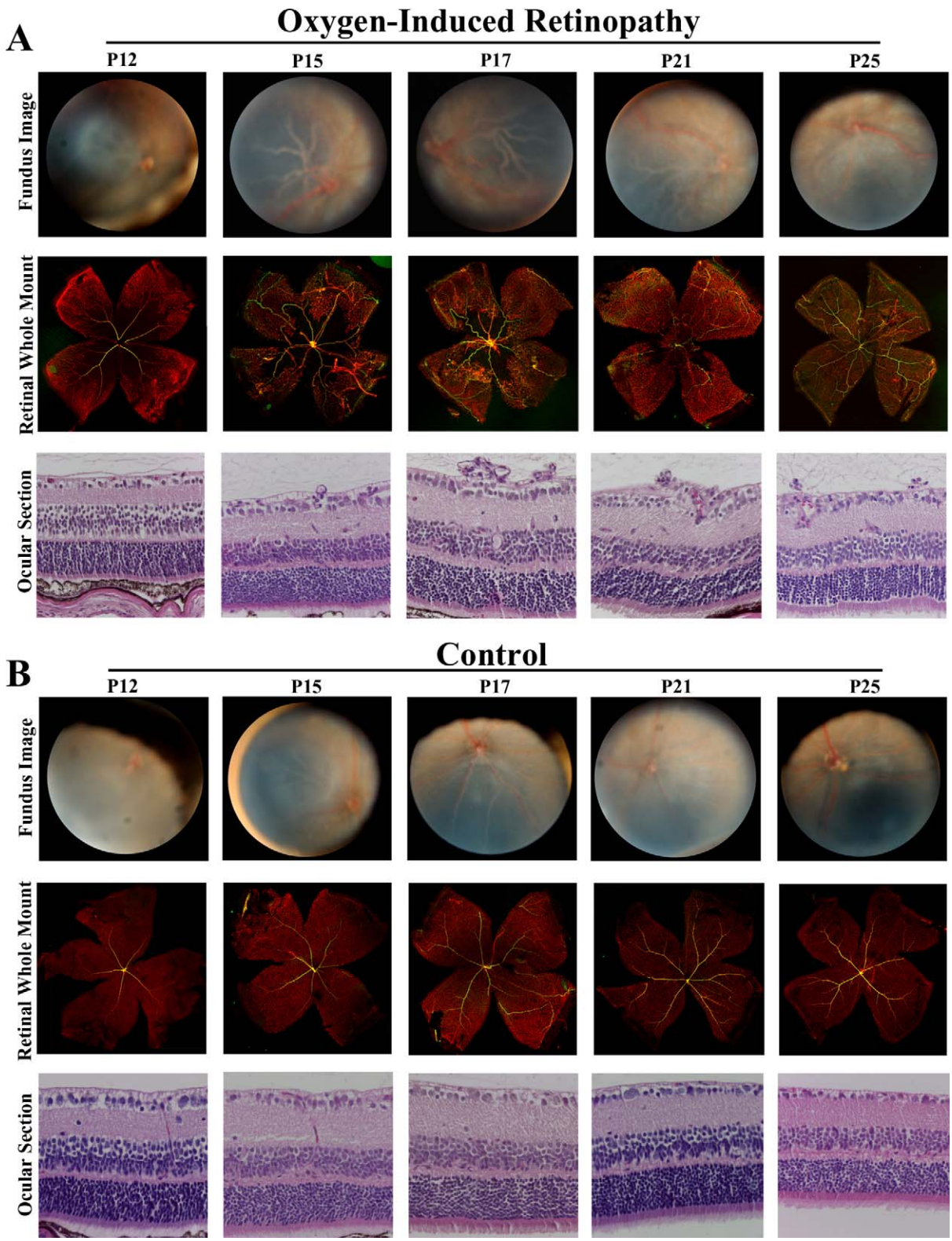

Figure 2. Oxygen-induced retinopathy in C57/BL6 mice. Representative retinal images obtained by TEFI at P12, P15, P17, P21, and P25, with eye-matched ocular cross sections stained to show neovascular nuclei (hematoxylin and eosin, original magnification: 400X) and retinal whole mounts stained to identify avascular retina (isolectin GS-IB4 Alexa Fluor 647 [vascular endothelium: red] and anti-mouse alpha smooth muscle antibody Cy3 [identifying arteries: yellow], original magnification: 40X).

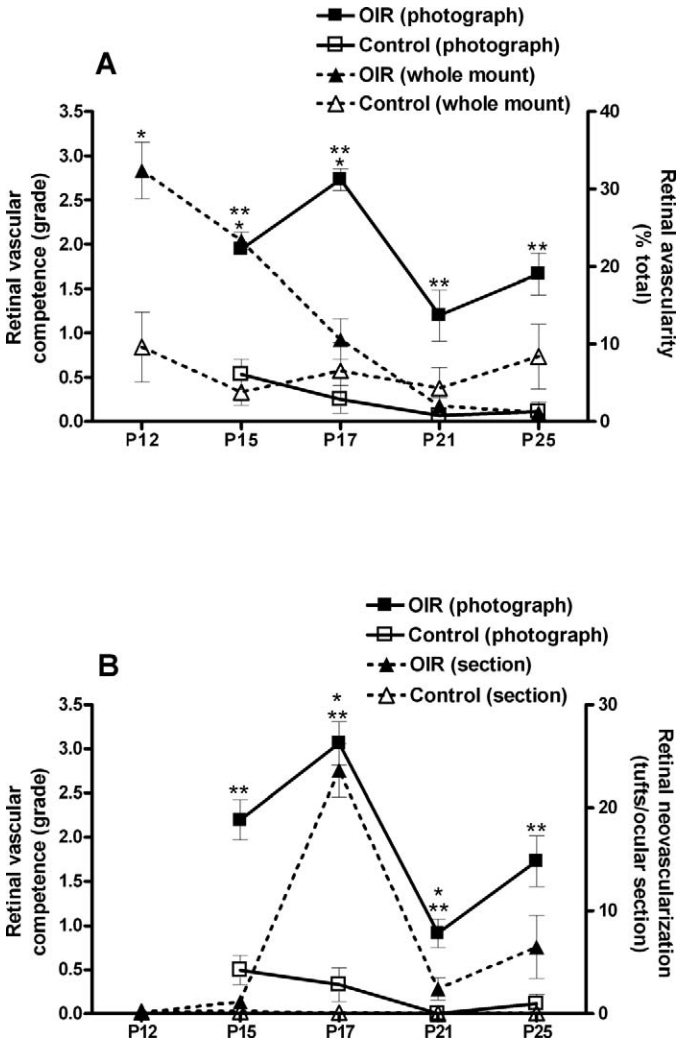

Figure 3. Comparison of retinal vascular competence grade by TEFI with vaso-obliteration in retinal whole mounts and retinal neovascularization in ocular cross sections in oxygen-induced retinopathy. (A) Graph showing retinal vascular competence assigned to retinal photographs and retinal avascularity measured on whole mounts from mice with oxygen-induced retinopathy or nondiseased control animals at P15, P17, P21, and P25 (n = three to six right eyes per group) and (B) graph showing retinal vascular competence assigned to retinal photographs and retinal neovascularization quantified in ocular cross sections from mice with oxygen-induced retinopathy or nondiseased control animals at P15, P17, P21, and P25 (n = three to six left eyes per group). Error bars = standard error of mean. Retinal vascular competence score for each eye is the mean score generated from three graders. (A) * = $P < 0.05$ for avascular retina between mice with oxygen-induced retinopathy and control mice; (B) * = $P < 0.05$ for retinal neovascular tufts between mice with oxygen-induced retinopathy and control mice; (A, B) ** = $P < 0.05$ for retinal vascular competence grade between mice with oxygen-induced retinopathy and control mice. Statistical analysis by Student's t-test, two-tailed.

lar incompetence became more pronounced in mice with oxygen-induced retinopathy (grade mean ± standard error of mean in diseased vs. control animals: 2.90 ± 0.09 vs. 0.29 ± 0.14; n = four or five mice per group; $P < 0.0001$; Student's t-test). As the mice aged, vascular incompetence was reduced in severity, although still present through P25 (grade mean ± standard error of mean in diseased vs. control animals: P21, 1.07 ± 0.20 vs. 0.03 ± 0.03; n = five mice per group; $P = 0.001$; P25, 1.70 ± 0.22 vs. 0.11 ± 0.06; n = three to five mice per group; $P = 0.002$; Student's t-test).

We compared the clinical observations made by TEFI to results of standard postmortem retinal evaluations in mice with oxygen-induced retinopathy versus age-matched control animals; retinal vaso-obliteration was measured in whole mounts with labeled vasculature, and retinal neovascularization was quantified in hematoxylin- and eosin-stained ocular cross sections (Fig. 3). When measured according to severity, retinal vaso-obliteration preceded retinal vascular incompetence. The area of avascular retina was significantly larger in diseased mice at P12 through P17 ($P \leq 0.012$; Student's t-test), with a decrease across these time points, and became no different by P21 through P25 ($P > 0.05$) (Fig. 3A). In contrast, the peak of retinal neovascularization coincided with maximum retinal vascular incompetence, although the former resolved whereas the latter persisted over the study period. Mice with oxygen-induced retinopathy demonstrated significant retinal neovascularization that peaked at P17 and was also present at P21 ($P \leq 0.008$; Student's t-test), but was not significant at P12 and P15, or at P25 ($P > 0.05$) (Fig. 3B).

Graders who scored the photographic images obtained by TEFI were blinded to the age of mice and used standard photographs to give scores. The weighted Fleiss-Cohen kappa indicated good agreement for retinal vascular competence scores for the same images across the three graders ($\kappa = 0.63$–0.78), indicating low interobserver variation with the defined scoring system. Consistent with this result, there was no significant difference in scores assigned by the three graders to eyes of mice from each of the four postnatal ages that were satisfactorily imaged, in either diseased or control groups ($P > 0.05$, ANOVA). The weighted Fleiss-Cohen kappa also demonstrated good intraobserver agreement for all graders ($\kappa = 0.70$–0.76). Scores for the three graders are compared in Figure 4.

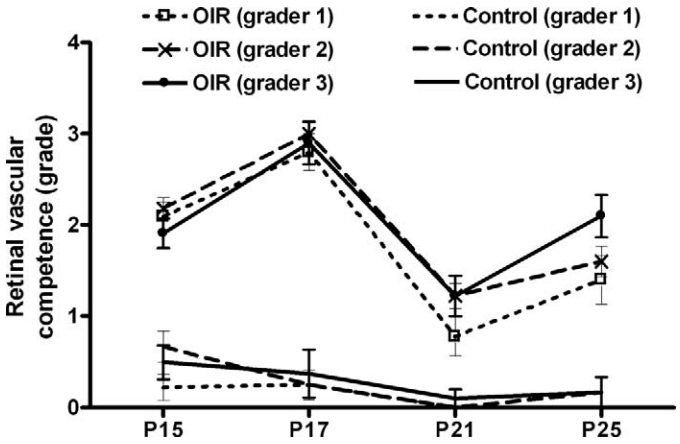

Figure 4. Interobserver agreement on scoring TEFI retinal photographs. Graph comparing mean retinal vascular competence scores given by three masked graders for retinal photographs obtained by TEFI from mice with oxygen-induced retinopathy or nondiseased control mice at P15, P17, P21, and P25. Error bars = standard error of mean; $n = 6$ to 11 eyes per group. There were no significant differences ($P > 0.05$, ANOVA) in scores given between the three graders at any time point for either group of mice. Weighted Fleiss-Cohen kappa for scores of same images across the three graders indicated good agreement ($\kappa = 0.63$–0.78).

Discussion

Retinopathy of prematurity is evaluated in neonates by clinical ophthalmic examination with indirect ophthalmoscopy, and increasingly, this evaluation is complemented by photographic documentation of the retina. In contrast, for the well-established mouse model of oxygen-induced retinopathy, studies of eye pathology are conducted postmortem, with the retina assessed for vaso-obliteration and neovascularization. In this study, we show that intravital fundus imaging may be applied to define another aspect of oxygen-induced retinopathy, that is, retinal vascular incompetence in the form of retinal vascular tortuosity and dilatation, which is not apparent in age-matched room air control pups. Using TEFI, we demonstrate that retinal vascular changes are present from P15, when imaging first becomes possible. The changes peak in severity at P17, and are reduced, but persistent through P25. In addition, we show that it is possible to grade retinal vascular competence using a 5-point system, with good intra- and interobserver agreement. Comparison with standard in vitro tissue analyses to determine retinal vaso-obliteration and neovascularization indicates that retinal vascular incompetence peaks after avascularity begins to decrease in area and coincident with the maximum of neovascularization.

Both retinopathy of prematurity and oxygen-induced retinopathy are initiated by relative retinal hyperoxia, resulting from premature exposure to the extrauterine environment and compounded by the use of supplementary oxygen therapy.[1] Normal vascular development is halted and relative hypoxia ensues; VEGF is upregulated and, in the presence of insulin-like growth factor-1, induces the growth of pathological retinal vessels.[20] Vascular endothelial growth factor also induces vascular dilatation and leakage.[21] Retinal vessel dilatation and tortuosity is a prominent feature of retinopathy of prematurity; this loss of retinal vascular competence is referred to as "pre-plus" or "plus" disease, depending on the severity, when it involves the posterior pole.[13,22] Our findings agree with reported observations of retinal arteriolar and venular tortuosity by fundus camera in the less commonly employed rat model of oxygen-induced retinopathy.[23] The TEFI results showed that the mouse retina does not return to normal by P25, which is usually considered to represent the postnatal age of regressed disease.[11] This is consistent with observations in neonates, who may experience persistent retinal vascular abnormalities after regression of retinopathy of prematurity, including abnormal retinal vascular branching, tortuosity, telangiectasias, and straightening and dragging of the retinal vessels.[24,25]

The International Classification of Retinopathy of Prematurity[13,22,24] was originally described as a standardized method by which ophthalmologists might grade disease at the bedside, and in middle-income countries where retinopathy of prematurity is most prevalent today, it continues to be used in this way. However, it is now clear that there may be considerable intra- and interobserver disagreement in the identification of plus disease.[26] This is a major concern, since the correct and well-timed identification of a plus disease finding is essential for the optimum management of sight-threatening retinopathy of prematurity. Consequently, there has been considerable interest in using computer-based image analysis to improve the definition and identification of plus disease.[27] The retinal photographs obtained by TEFI readily lend themselves to such analysis, although in this study, we sought to establish a simple clinical grading method that would not raise the otherwise low cost of the system. Comparison between the three graders by weighted Fleiss-Cohen kappa indicated we had achieved this. Our graders

received no training, but were supplied with standard photographs and definitions. It should be further noted that one of the graders was a basic scientist with no clinical experience; this individual's performance was comparable to that of the other two graders, who, as experienced vitreoretinal surgeons, routinely managed retinopathy of prematurity.

Several technical considerations warrant discussion specifically in relation to using TEFI for imaging retinal vascular changes in oxygen-induced retinopathy. The small eye, incomplete or absent lid opening, and media opacity in the mouse at P12 preclude imaging at this time point. Imaging of the retinal periphery is limited at P15, but readily performed from P17. However, while the acquisition of peripheral images may be important in experimental models of other diseases, such as uveitis, since vascular changes appear similar in the periphery and at the posterior pole in oxygen-induced retinopathy, we suggest that a posterior pole photograph is sufficient for grading purposes. We used a high ISO (i.e., 800–1600) and a slow shutter speed (i.e., 0.1–0.2 s) to compensate for the small pupil diameter in the pups to bolster the brightness of the image. Certain characteristic findings in retinopathy of prematurity, including the demarcation line, ridge, and extraretinal fibrovascular proliferation, are not seen with TEFI, which reflects the limit of resolution of the system at least in relation to fibrovascular proliferation. Modifications, such as the use of red-free filter imaging, infrared imaging, and/or a combination with fluorescein angiography, might facilitate visualization of retinal neovascularization, albeit at increased cost. Although conscious mice may be imaged with TEFI,[14] we prefer the use of general anesthesia in this setting.

In summary, we have used TEFI, which is a form of intravital imaging, to demonstrate clinical signs of retinal vascular incompetence in mice with oxygen-induced retinopathy. These animals exhibit retinal vascular dilatation and tortuosity, and in extreme cases, vitreous hemorrhage, with severity peaking as retinal neovascularization also reaches its maximum extent. The method provides color fundus photographs of sufficient quality for grading in mice aged P15 or older, and our simple five-grade clinical scoring system is reproducible for persons with and without a background in the clinical evaluation of retinopathy of prematurity. In addition, TEFI provides an opportunity for multiple retinal evaluations in the same mouse over the course of the disease. From a practical perspective, the equipment required for the system is very inexpensive, costing a total of $5000 to $6000. As an accurate and cost-efficient method, TEFI is an appealing complement to standard postmortem analyses for following the course of oxygen-induced retinopathy, with obvious application in studies of pathogenesis and the evaluation of novel biologic drugs for retinopathy of prematurity.

Acknowledgments

The authors thank Heping Xu, PhD (Queen's University Belfast, Belfast, United Kingdom), for expert advice and Andre Cherri for technical assistance.

This research was supported in part by funding from the National Eye Institute of the National Institutes of Health (R01 EY019042 [BA], R01 EY011548 [MRP], P30 EY010572 [DC]), Research to Prevent Blindness (unrestricted grant to Casey Eye Institute), and the Casey Eye Institute VISION 2020 International Fellowship Program (JMF).

Disclosure: **J.M. Furtado,** None; **M.H. Davies,** None; **D. Choi,** None; **A.K. Lauer,** None; **B. Appukuttan,** None; **S.T. Bailey,** None; **H.T. Rahman,** None; **J.F. Payne,** None; **A.J. Stempel,** None; **K. Mohs,** None; **M.R. Powers,** None; **S. Yeh,** None; **J.R. Smith,** None

References

1. Sapieha P, Joyal JS, Rivera JC, et al. Retinopathy of prematurity: understanding ischemic retinal vasculopathies at an extreme of life. *J Clin Invest*. 2010;120:3022–3032.
2. Gilbert C. Retinopathy of prematurity: a global perspective of the epidemics, population of babies at risk and implications for control. *Early Hum Dev*. 2008;84:77–82.
3. Rahi JS, Gilbert CE, Foster A, Minassian D. Measuring the burden of childhood blindness. *Br J Ophthalmol*. 1999;83:387–388.
4. Gilbert C. Blindness in children. In: International Agency for the Prevention of Blindness: 2010 Report; 2010:73–75.
5. Early Treatment for Retinopathy of Prematurity Cooperative Group. Revised indications for the treatment of retinopathy of prematurity: results

of the early treatment for retinopathy of prematurity randomized trial. *Arch Ophthalmol*. 2003; 121:1684–1694.
6. Good WV, Hardy RJ, Dobson V, et al. Final visual acuity results in the early treatment for retinopathy of prematurity study. *Arch Ophthalmol*. 2010;128:663–671.
7. Simpson JL, Melia M, Yang MB, Buffenn AN, Chiang MF, Lambert SR. Current role of cryotherapy in retinopathy of prematurity: a report by the American Academy of Ophthalmology. *Ophthalmology*. 2012;119:873–877.
8. Micieli JA, Surkont M, Smith AF. A systematic analysis of the off-label use of bevacizumab for severe retinopathy of prematurity. *Am J Ophthalmol*. 2009;148:536–543;e532.
9. Smith LE, Wesolowski E, McLellan A, et al. Oxygen-induced retinopathy in the mouse. *Invest Ophthalmol Vis Sci*. 1994;35:101–111.
10. Aguilar E, Dorrell MI, Friedlander D, et al. Chapter 6. Ocular models of angiogenesis. *Methods Enzymol*. 2008;444:115–158.
11. Stahl A, Connor KM, Sapieha P, et al. The mouse retina as an angiogenesis model. *Invest Ophthalmol Vis Sci*. 2010;51:2813–2826.
12. Connor KM, Krah NM, Dennison RJ, et al. Quantification of oxygen-induced retinopathy in the mouse: a model of vessel loss, vessel regrowth and pathological angiogenesis. *Nat Protoc*. 2009; 4:1565–1573.
13. International Committee for the Classification of Retinopathy of Prematurity. The International Classification of Retinopathy of Prematurity revisited. *Arch Ophthalmol*. 2005;123:991–999.
14. Paques M, Guyomard JL, Simonutti M, et al. Panretinal, high-resolution color photography of the mouse fundus. *Invest Ophthalmol Vis Sci*. 2007;48:2769–2774.
15. Copland DA, Wertheim MS, Armitage WJ, Nicholson LB, Raveney BJ, Dick AD. The clinical time-course of experimental autoimmune uveoretinitis using topical endoscopic fundal imaging with histologic and cellular infiltrate correlation. *Invest Ophthalmol Vis Sci*. 2008;49: 5458–5465.
16. Xu H, Koch P, Chen M, Lau A, Reid DM, Forrester JV. A clinical grading system for retinal inflammation in the chronic model of experimental autoimmune uveoretinitis using digital fundus images. *Exp Eye Res*. 2008;87:319–326.
17. Davies MH, Stempel AJ, Hubert KE, Powers MR. Altered vascular expression of EphrinB2 and EphB4 in a model of oxygen-induced retinopathy. *Dev Dyn*. 2010;239:1695–1707.
18. Fleiss JL, Cohen J, Everitt BB. Large sample standard errors of kappa and weighted kappa. *Psychol Bull*. 1969;72:332–327.
19. Altman DG. *Practical Statistics for Medical Research*. London: Chapman and Hall; 1991.
20. Hellstrom A, Perruzzi C, Ju M, et al. Low IGF-I suppresses VEGF-survival signaling in retinal endothelial cells: direct correlation with clinical retinopathy of prematurity. *Proc Natl Acad Sci U S A*. 2001;98:5804–5808.
21. Otrock ZK, Makarem JA, Shamseddine AI. Vascular endothelial growth factor family of ligands and receptors: review. *Blood Cells Mol Dis*. 2007;38:258–268.
22. Committee for the Classification of Retinopathy of Prematurity. An international classification of retinopathy of prematurity. *Arch Ophthalmol*. 1984;102:1130–1134.
23. Liu K, Akula JD, Falk C, Hansen RM, Fulton AB. The retinal vasculature and function of the neural retina in a rat model of retinopathy of prematurity. *Invest Ophthalmol Vis Sci*. 2006;47: 2639–2647.
24. International Committee for the Classification of the Late Stages of Retinopathy of Prematurity. An international classification of retinopathy of prematurity. II. The classification of retinal detachment. *Arch Ophthalmol*. 1987;105:906–912.
25. Preslan MW, Butler J. Regression pattern in retinopathy of prematurity. *J Pediatr Ophthalmol Strabismus*. 1994;31:172–176.
26. Wallace DK, Quinn GE, Freedman SF, Chiang MF. Agreement among pediatric ophthalmologists in diagnosing plus and pre-plus disease in retinopathy of prematurity. *J AAPOS*. 2008;12: 352–356.
27. Wittenberg LA, Jonsson NJ, Paul Chan RV, Chiang MF. Computer-based image analysis for plus disease diagnosis in retinopathy of prematurity. *J Pediatr Ophthalmol Strabismus*. 2012;49: 11–19.